National Aeronautics and Space Administration

Physics of Failure Analysis of Xilinx Flip Chip CCGA Packages: Effects of Mission Environments on Properties of LP2 Underfill and ATI Lid Adhesive Materials

Jong-ook Suh
Jet Propulsion Laboratory
Pasadena, California

Jet Propulsion Laboratory
California Institute of Technology
Pasadena, California

JPL Publication 13-8 04/13

National Aeronautics and Space Administration

Physics of Failure Analysis of Xilinx Flip Chip CCGA Packages: Effects of Mission Environments on Properties of LP2 Underfill and ATI lid Adhesive Materials

NASA Electronic Parts and Packaging (NEPP) Program
Office of Safety and Mission Assurance

Jong-ook Suh
Jet Propulsion Laboratory
Pasadena, California

NASA WBS: 724297.40.49.11
JPL Project Number: 104593
Task Number: 40.49.02.13

Jet Propulsion Laboratory
4800 Oak Grove Drive
Pasadena, CA 91109

http://nepp.nasa.gov

This research was carried out at the Jet Propulsion Laboratory, California Institute of Technology, and was sponsored by the National Aeronautics and Space Administration Electronic Parts and Packaging (NEPP) Program.

Reference herein to any specific commercial product, process, or service by trade name, trademark, manufacturer, or otherwise, does not constitute or imply its endorsement by the United States Government or the Jet Propulsion Laboratory, California Institute of Technology.

©2013 California Institute of Technology. Government sponsorship acknowledged.

TABLE OF CONTENTS

1.0 Introduction 1
2.0 Properties of the LP2 underfill material 2
2.1 Mechanical and viscoelastic properties of the LP2 underfill 2
2.1.1 Effect of filler settling on the elastic modulus of the LP2 underfill 2
2.1.2 Elastic modulus of the LP2 underfill as function of temperature 4
2.1.3 Low-frequency DMA test response of the LP2 underfill 7
2.2 Effect of environmental exposure to properties of the LP2 underfill 9
2.2.1 Effect of long-term vacuum and humidity exposure to adhesive strength of the LP2 underfill 9
2.2.2 Effect of long-term vacuum and humidity exposure to viscoelastic and thermal expansion behavior of the LP2 underfill 10
3.0 Properties of ATI lid adhesive material 14
3.1 Outgassing properties of the ATI material 14
3.2 Effect of environmental exposure to properties of the ATI lid adhesive material 15
3.2.1 Effect of long-term vacuum and humidity exposure to adhesive strength of the ATI lid adhesive 15
3.2.2 Effect of long-term vacuum and humidity exposure to viscoelastic and thermal expansion behavior of the ATI lid adhesive material 16
3.2.3 Effect of long-term vacuum and humidity exposure to Thermal conductivity of the ATI material 19
4.0 Summary 20
5.0 References 21

1.0 INTRODUCTION

The Xilinx Virtex 4QV and 5QV (V4 and V5) are next-generation, reconfigurable, SRAM-based, field-programmable gate arrays (FPGAs). Due to their reconfigurability, performance, and radiation tolerance, they are strong candidates for use on future NASA flight projects. Schematically depicted in Figure 1-1, V4 and V5 virtually have the same packaging configuration: the flip chip die is mounted on an alumina substrate with 95Pb5Sn flip chip solder bumps, the SiC lid is attached to the die for heat management, and the 90Pb10Sn solder columns are attached to the substrate. Except for presence of the solder columns, this structure resembles the traditional IBM C4 ceramic substrate flip chip structure, which has been proven reliable in mainframe computer applications. While this structure would seem to be a natural choice for parts manufacturers when packaging high-density, integrated circuit devices, the space community has raised concerns about its reliability, as this structure is non-hermetic. Typically for commercial applications, an underfilled flip chip package does not require hermetic packaging because the underfill provides adequate environmental protection to the interconnections. However, this type of non-hermetic packaging does not meet space application standards because the polymer materials, such as the underfill and lid adhesive, are directly exposed to the space environment. At this time, V5 type packages are not qualified to MIL-PRF-38535 Qualified Manufacturer Listing (QML) Level V, due to their non-hermeticity. There is currently an activity to setup a new Class Y for non-hermetic space parts to provide QML coverage for Xilinx V5 type devices.

V4 and V5 not only share the same packaging structure, but they also share same underfill (LP2) and lid adhesive (ATI) material. Since both LP2 underfill and ATI lid adhesive materials are directly exposed to the space environment, their properties, and how they interact with the spacecraft environment, must be investigated. There are many constituents of the low Earth orbit (LEO) environment: high vacuum, ionizing radiation, atomic oxygen, UV radiation, etc. Electronics within a spacecraft are protected by shielding and exposed to less harsh conditions than outside, and long-term vacuum exposure is the most realistic environmental concern for the LP2 underfill material used in non-hermetic V4/V5 packages.

In FY11, JPL conducted an extensive study on the reliably of the LP2 underfill material used in both V4 and V5. The purpose of FY12 study presented in this report is to continue investigating reliability concerns associated with the non-hermeticity of V4/V5 packages. This study mainly focuses on the effects of environmental exposure to the underfill and the lid adhesive.

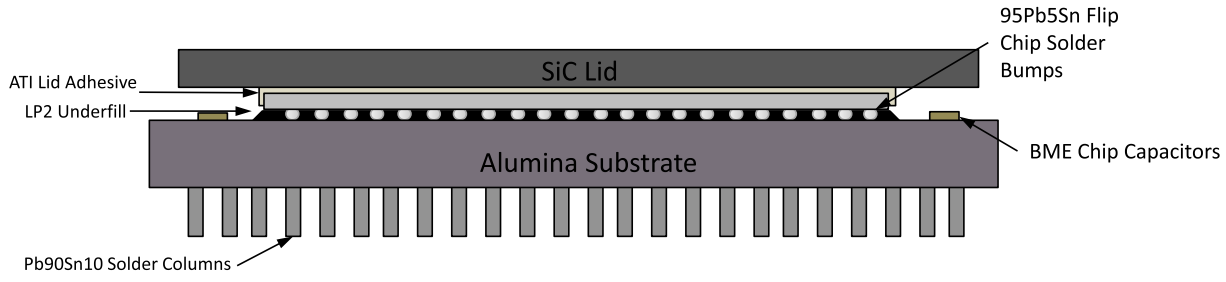

Figure 1-1. Schematic structure of Xilinx V4/V5 packages.

2.0 PROPERTIES OF THE LP2 UNDERFILL MATERIAL

In FY11, we investigated the basic properties of the LP2 underfill material and confirmed that its properties—glass-transition temperature (Tg), coefficient of thermal expansion (CTE), Young's modulus, and adhesive strength—are suitable for high-reliability ceramic flip chip package applications [1]. The LP2 underfill material exhibited high lap shear strength under a wide range of temperatures relevant to space applications and good outgassing reliability under both vacuum thermal cycling and radiation environments. The LP2 underfill did not show any significant weakness from tests done under atmospheric pressure. In order to study its reliability in the mission environment, we investigated how environmental exposures, such as long-term vacuum exposure and humidity exposure, affect the properties of the LP2 material. However, we must note that this type of approach has limitations, because how changes in properties of the materials containing the package would translate to reliability of the actual package cannot be accurately assessed unless real packages are used as samples. consisting

2.1 Mechanical and viscoelastic properties of the LP2 underfill

The elastic modulus is one of the most important properties of underfill material. It should be large enough to take over the stress from solder bumps without exerting excessive stress on the die. The correct value of the elastic modulus is crucial when performing finite element analysis (FEA) to identify stress level or stress distribution within flip chip solder bumps. In addition, it is necessary to know the elastic modulus of the underfill over a wide range of temperatures, to simulate the environments to which spacecraft electronic assemblies are exposed. In FY11, elastic modulus of the underfill measured by nanoindentation was about 9 to 11 GPa [1]. The measurements were done on surfaces of 2 mm thick bulk underfill samples, at the room temperature. In this study, we investigated the effects of temperature and filler settling on the elastic modulus of the LP2 underfill.

2.1.1 Effect of filler settling on the elastic modulus of the LP2 underfill

Figure 2.1.1-1 shows cross-sectional SEM images of a V4 package where the filler settling is noticeable. The die side of the underfill is richer with soft resin, while the substrate side has a greater concentration of filler particles. The filler settling is a known issue in flip chip packaging and generally considered undesirable. It will result in inconsistency of properties along the thickness of the underfill. The filler-rich region is expected to be stiffer and have lower CTE. The CTE of the LP2 underfill measured by TMA was 21.27 ppm/°C, and CTEs at the filler-rich and resin-rich regions were estimated to be 13 ppm/°C and 26 ppm/°C, respectively [1]. The resin-rich region is expected to be more compliant and have higher CTE. It is necessary to know how property varies according to location within the underfill layer to perform precise FEA.

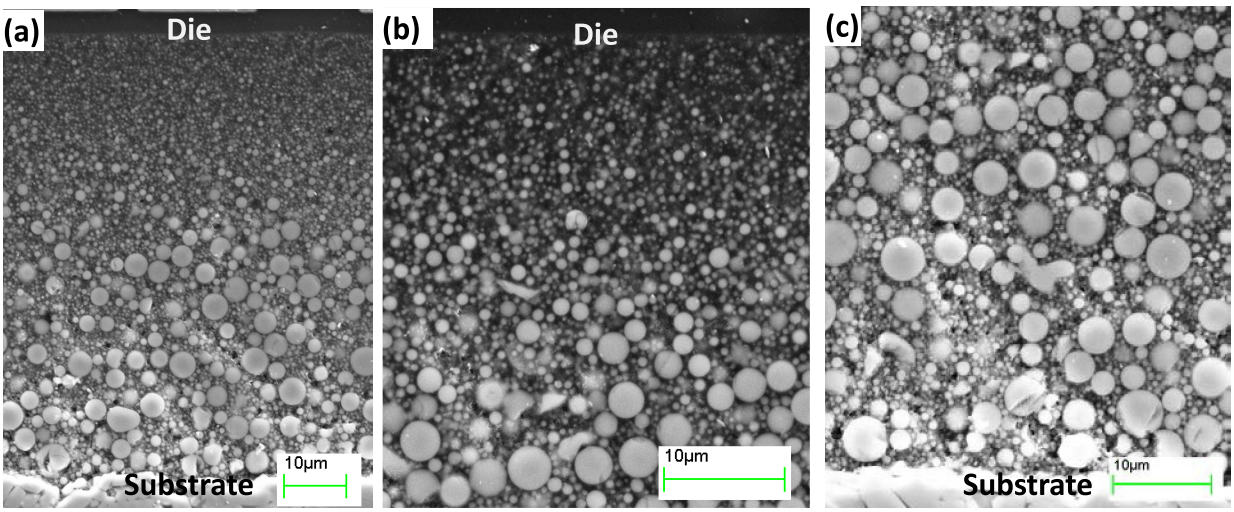

Figure 2.1.1-1. Micrograph of a V4 package cross-section showing the filler settling of the LP2 underfill: (a) entire view across the thickness of the underfill; (b) enlarged view of the die side; and (c) enlarged view of the substrate side.

The elastic modulus of the LP2 material measured by nanoindentor during the FY11 task was about 9 to 11 GPa [1]. The measurement was done on surfaces of 2 mm thick bulk underfill samples. Measurements were performed on the top surfaces; therefore, the measured elastic modulus might have been affected by the filler settling, if the filler settling had taken place during sample preparation.

Figure 2.1.1-2 is a cross-sectional micrograph of the 2 mm thick LP2 material. The filler settling took place in the sample. In order to confirm the previous measurement, and to precisely predict behavior of the Xilinx CCGA packages, elastic modulus of the LP2 material was measured according to its location. The 2 mm thick bulk sample and a V4 package were cross-sectioned and polished prior to nanoindentation. For the 2 mm thick bulk sample, nanoindentations were done on the top, middle, and bottom of the sample. For the cross-sectioned V4 package, measurements were done on the underfill layer just below the die, middle, and right above the substrate. The strain rate was 0.05/sec, and the indentation depth was 2 μm. Note that the definition of the strain rate in the nanoindentation is different from strain rate in the tensile or shear test; the strain rate here is produced under the indenter.

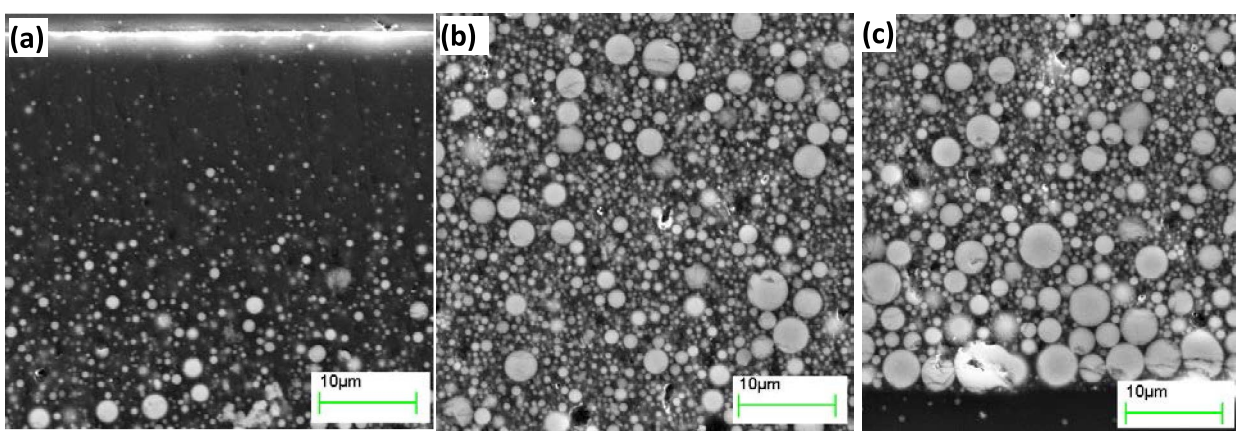

Figure 2.1.1-2. Micrograph of a 2mm thick bulk LP2 underfill material specimen cross-section: (a) top side, (b) middle, and (c) bottom side of the specimen.

The measured elastic modulus is shown in Table 2.1.1-1. The die side has a lower elastic modulus than the center and substrate side.

Table 2.1.1-1. Elastic modulus measured by nanoindentation of the LP2 underfill, according to the location.

Underfill Location	Elastic modulus, measured from a cross-sectioned V4 package	Elastic modulus, measured from a cross-sectioned bulk LP2 sample
Die/top side (0.05/sec strain rate)	6.5GPa	10.2GPa
Middle (0.05/sec strain rate)	12.1GPa	12.9GPa
Substrate/bottom side (0.05/sec strain rate)	12.1GPa	13.6GPa
Middle (0.005/sec strain rate)	9.7 GPa	10.2 GPa

Since the underfill material is a viscoelastic material, the apparant elastic modulus is affected by the strain rate. Therefore, the strain rate of the nanoindentation was lowered to 0.005/sec to see if there is any effect of the strain rate. Indentations were only done at the middle of the underfill. The apparent elastic modulus decreased when the strain rate was lowered. The results are shown in the last row of Table 2.1.1-1. Both the cross-sectioned V4 package and the bulk LP2 samples exhibited about 20% reduction in the elastic modulus at a lower strain rate.

2.1.2 Elastic modulus of the LP2 underfill as function of temperature

In FY11, elastic modulus of the LP2 underfill was tested by nanoindentation. Nanoindentation was preferred over the tensile test in the FY11 study because nanoindentation did not require the preparation of dog-bone-shaped samples. One limitation of the FY11 nanoindentation was that the nanoindentation machine was not capable of conducting tests at different temperatures. In the FY12 study, elastic modulus of the LP2 material was measured under different temperatures using specimens constructed per ASTM D638, as shown in Figure 2.1.2-1.

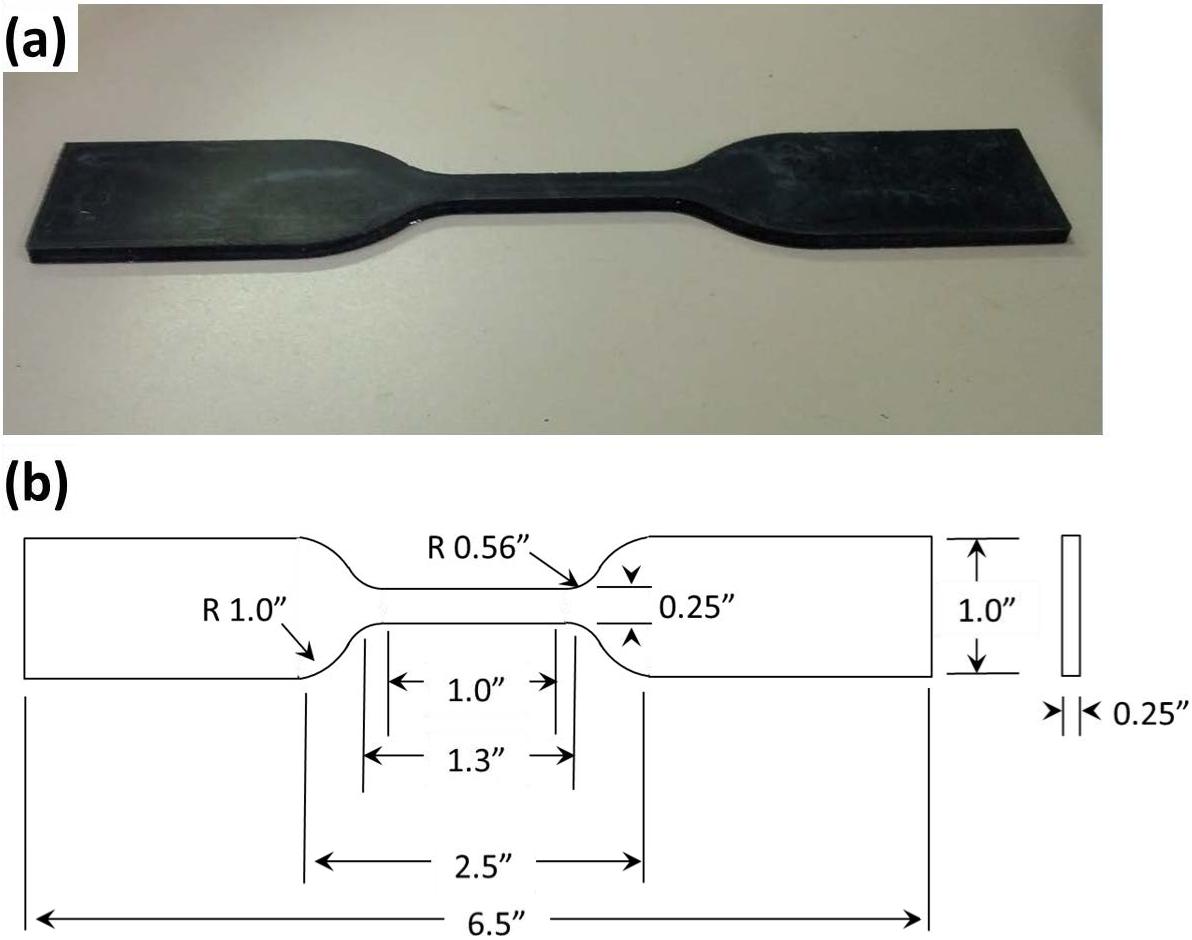

Figure 2.1.2-1. (a) Photograph of a dog-bone sample. (b) Dimension of the dog-bone samples.

Tensile tests were done under a strain rate of 8.3×10^{-5}/sec, at −55°C, +22°C, and +125°C. The tensile test machine was setup to provide the lowest strain rate the machine can produce, which is much lower than the suggested strain rate in the ASTM standard. The purpose was to reflect the actual strain rate that underfill material sees during thermal cycling. When a ceramic flip chip package is under thermal cycling with a ramp rate of 12°C/min, the strain rate of underfill is about 4×10^{-6}/sec [2]. Because the tensile test machine was not able to produce such a low strain rate, the machine was set to produce its lowest strain rate of 8.3×10^{-5}/sec. Five samples were measured at each temperature. Because dimensions varied slightly from sample to sample, dimension of each sample was measured prior to the test. Elongation of samples were measured through an extensometer attached to samples. Table 2.1.2-1 shows the measured elastic modulus and ultimate tensile strength of the LP2 underfill. The standard deviation of the tensile strength is large, which is common for a brittle material. Table 2.1.2-2 summarizes the elastic modulus of the LP2 underfill material. The elastic modulus measured at the room temperature is similar to the modulus measured by nanoindentation. It must be noted that the elastic modulus dropped down to 0.08 GPa at +125°C. Figure 2.1.2-2 shows selected stress strain curves at −55, +22, and +125°C. It must be also noted that there was a significant amount of noise in measurements done at +125°C, making it difficult to define the elastic modulus of the LP2 material. It is evident that the elastic moduls of the LP2 material will significantly decrease at +125°C; however, the 0.08 GPa seems too low because the storage modulus measured by dynamic mechanical analysis (DMA) in the following section did not significantly decrease at +125°C. Therefore, further investigation is required to varify such a low value of elastic modulus.

The Tg of LP2 underfill is known to be several tens of degrees higher than +125°C, according to thermomechanical analysis (TMA) and differential scanning calorimetry (DSC) [1]. Since the glass transition takes place over a range of temperatures, the above result indicates that the elastic modulus will start to decrease at a temperature well below +125°C.The present result suggests that the LP2 underfill material may not effectively reduce stress in flip chip solder bumps at higher temperatures. It would be necessary to measure elastic modulus at other temperatures to identify the temperature where the onset of the elastic modulus drop occurrs and how the elastic modulus changes according to temperature.

Table 2.1.2-1. Tensile test results of LP2 underfill measured at three different temperatures.

Test Temperature	Specimen Number	Modulus (GPa)	Ultimate Stress (MPa)
-55˚C	SN001	13.952	96.874
	SN002	12.029	27.385
	SN003	11.149	24.295
	SN004	14.118	41.752
	SN005	12.337	38.050
	Average	12.717	45.67
	STDEV	1.281	29.523
	COV %	10.073	64.643
Test Temperature	**Specimen Number**	**Modulus (GPa)**	**Ultimate Stress (MPa)**
22˚C	SN001	9.600	64.036
	SN002	10.302	52.247
	SN003	10.502	82.268
	SN004	10.306	75.659
	SN005	10.426	81.225
	Average	10.227	71.09
	STDEV	0.361	12.780
	COV %	3.526	17.978
Test Temperature	**Specimen Number**	**Modulus (GPa)**	**Ultimate Stress (MPa)**
+125˚C	SN001	0.114	3.677
	SN002	0.095	2.113
	SN003	0.056	4.034
	SN004	0.042	2.723
	SN005	0.093	4.133
	Average	0.080	3.34
	STDEV	0.030	0.882
	COV %	37.523	26.432

Table 2.1.2-2. Summary of the elastic modulus of the LP2 underfill measured at three different temperatures.

Temperature	Average Elastic Modulus (GPa)
−55°C	12.72
+22°C	10.23
+125°C	0.08

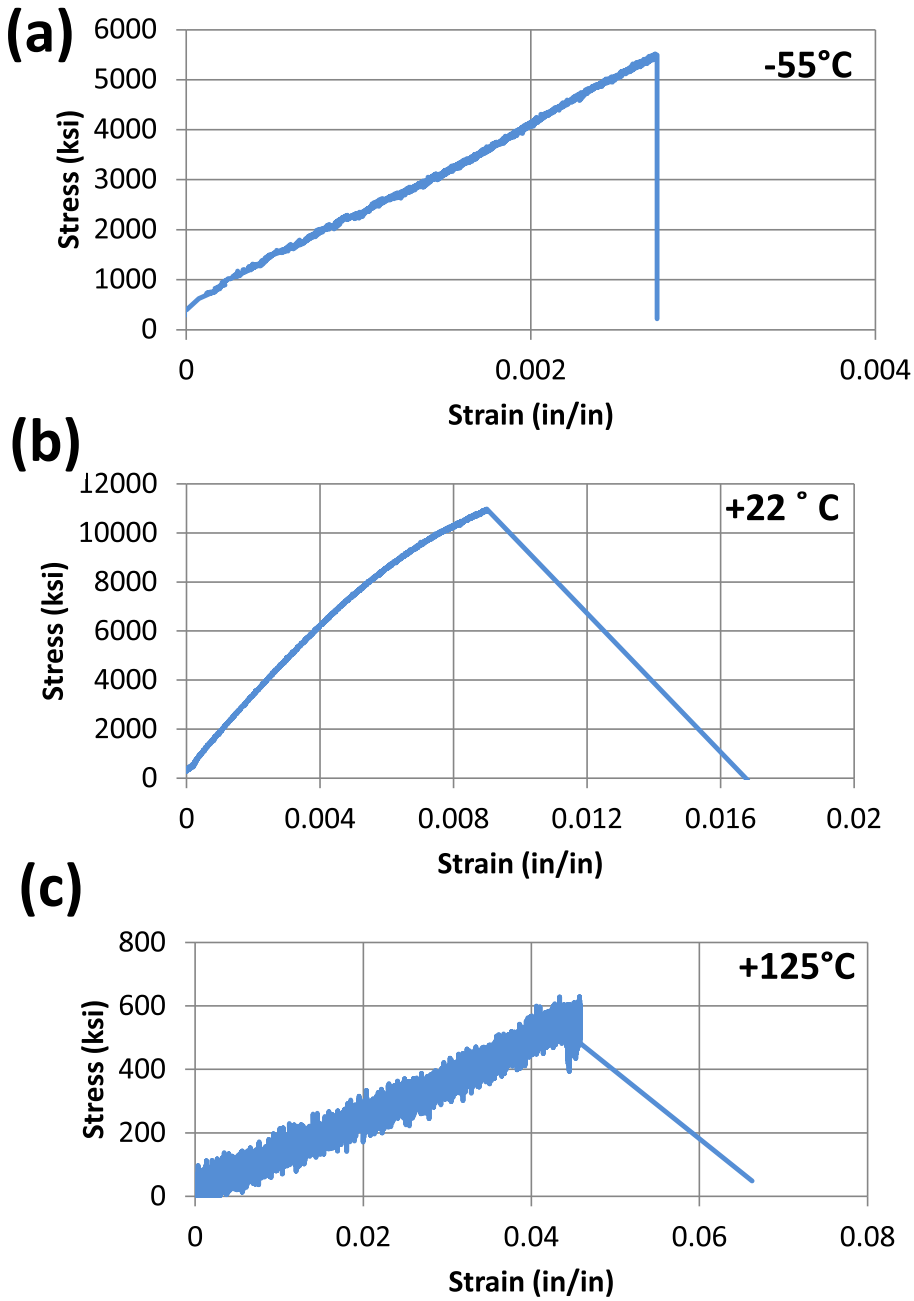

Figure 2.1.2-2. Stress-strain curves from tensile tests of dog-bone shape LP2 material samples, measured at (a) −55°C, (b) +22°C, and (c) +125°C.

2.1.3 Low-frequency DMA test response of the LP2 underfill

In FY11, DMA tests were conducted on bulk LP2 material samples [1]. DMA tests were performed in a single cantilever mode on bulk a rectangular LP2 sample, at a constant frequency (1 Hz) and constant amplitude (20 μm). The sample's width and thickness were about 10 mm and 2 mm, respectively. The distance between the two clamp mounts was 17.50 mm. In single cantilever bending, the strain rate of a sample is given as,

$$\varepsilon = 1.5 \times \frac{t\Delta}{L^2}.$$

Where t is the thickness of the sample, Δ is the displacement of the clamp, and L is the distance between the clamps. For the DMA test condition specified above, L is 17.50 mm, t is 2 mm, and the strain of the sample at the maximum amplitude (Δ=20 μm) is,

$$\varepsilon = 1.5 \times \frac{2mm \times 20 \times 10^{-3} mm}{17.5^2 mm^2} = 1.959 \times 10^{-4}.$$

If the frequency is 1 Hz, the time for a sample to see its maximum deflection is 1/4=0.25 sec. Therefore, the strain rate is,

$$\dot{\varepsilon} = \varepsilon / 0.25 = 7.836 \times 10^{-4} / \sec.$$

When a ceramic flip chip package is under thermal cycling with a ramp rate of 12°C/min, the strain rate of underfill is about 4×10^{-6}/sec [2]. Therefore, the strain rate above is more than two orders of magnitude higher than what the flip chip underfill sees during actual thermal cycling. Since the underfill material is a viscoelastic epoxy material, DMA results will depend on frequency of the test. At higher frequencies, a material behaves more similarly to an elastic material. The apparent storage modulus is known to increase as frequency increases. The temperature where the storage modulus (E') drops also depends on frequency. Therefore, a DMA test under the 4×10^{-6}/sec strain rate would be more relevant to the real application. The low strain rate was achieved by lowering the frequency and amplitude of the test.

DMA was performed on a TA Q800 DMA instrument configured with a single cantilever clamp and a Gas Cooling Accessory (GCA). Two scans were done on a sample with a width and thickness of 10.27 mm and 2.50 mm, respectively. Sample length, a fixed value equal to the distance between the two clamp mounts, was 17.50mm. The first scan was done under the conventional scan condition, run from a temperature around −145ºC (equilibrated and then held isothermal for five minutes) to a temperature around +210ºC using a heat ramp rate of 2ºC/min, at 1 Hz frequency and 10 μm amplitude. The second scan was done under a low frequency scan of 0.01 Hz and amplitude of 10 μm. While the 1 Hz scan was done continuously from −145°C to +210°C, the 0.01 Hz scan was done in a two-stage experiment, consisting of a low-temp region and a high-temp region. For the low-temp region the "Temperature Step/Frequency Sweep" method was used, starting from −145ºC and incrementally increasing the temperature by 15ºC after each modulus measurement, until reaching +65ºC. The high-temp region started at +70ºC and was incrementally increased by 10ºC after each modulus measurement, until reaching +210ºC. The 0.01 Hz, 10 μm scan provided strain rate of

$$\dot{\varepsilon} = \varepsilon / 25\sec = 1.5 \times \frac{t\Delta}{L^2} \times \frac{1}{25\sec} = 1.5 \times \frac{2.5mm \times 10 \times 10^{-3} mm}{17.5^2 mm^2} \times \frac{1}{25\sec} = 4.898 \times 10^{-6} / \sec.$$

Figure 2.1.3-1 shows DMA results of the two scans. The storage and loss moduli, and tan delta for these two frequency experiments, are plotted in the figure. The 1 Hz scan is plotted with solid lines and the 0.01 Hz scan is plotted with dashed lines. It was found that at the lower frequency (i.e., 0.01 Hz), the onset of the storage modulus drop occurred around 10°C lower (~115°C vs. ~125°C), while the loss modulus peak was approximately 15°C lower (~120°C vs. ~135°C). The tan delta was found to follow this same trend, where the peak value was at a lower temperature (~135°C) for the low frequency sample relative to the higher frequency sample (~150°C). In general, E' tends to reduce as frequency reduces. E' showed slight decrease at the lower frequency in this test.

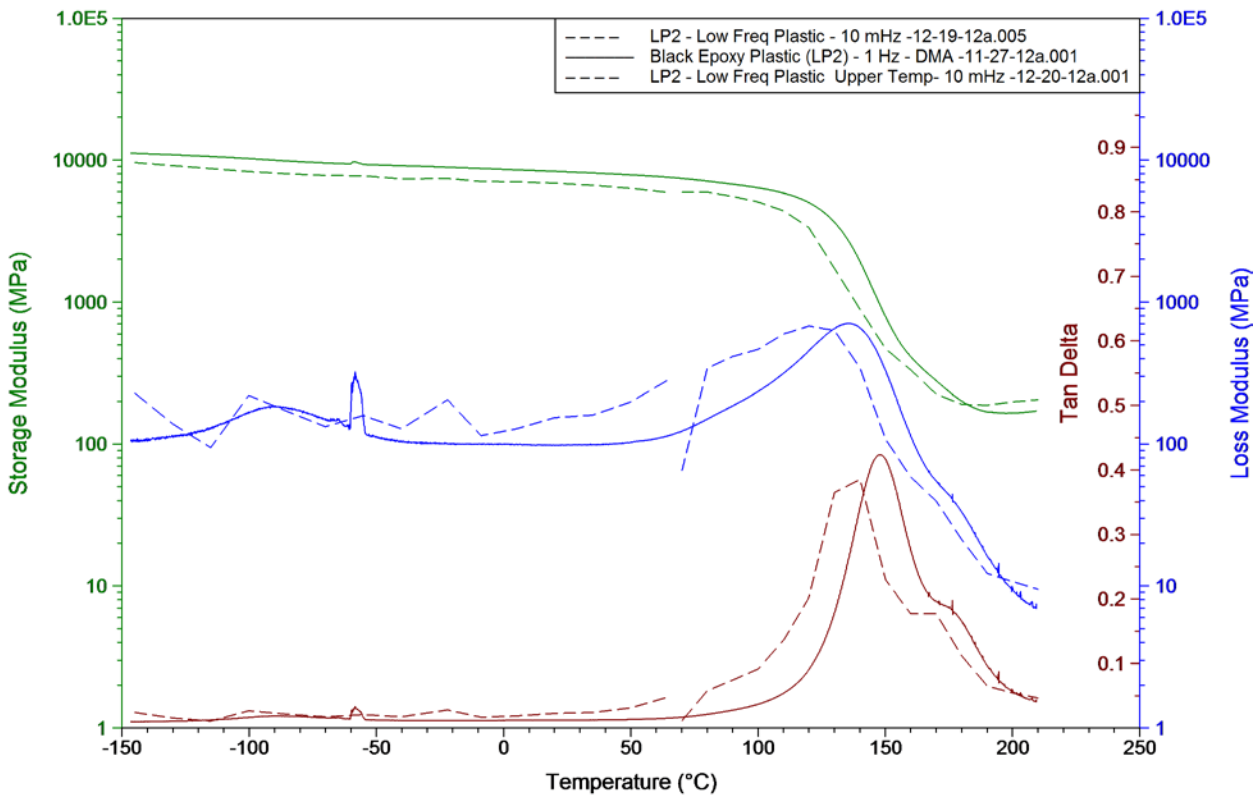

Figure. 2.1.3-1. DMA result of the LP2 underfill material sample at frequencies of 1 Hz (solid) and 0.01 Hz (dashed).

2.2 Effect of environmental exposure to properties of the LP2 underfill

Due to the non-hermeticity of the Xilinx CCGA packages, the LP2 underfill must be expected to interact with the spacecraft environment. It will also be exposed to the humid environment at Earth. In FY11, we made assessments on how various constituents of the space environment will threat reliability of the LP2 underfill. Due to the shielding practices, electronics within a spacecraft are exposed to less harsh conditions than outside of the spacecraft. Among all the constituents of the LEO environment, the long-term vacuum exposure was rated as the most realistic environmental concern for the LP2 underfill material. In the FY12 study, effects of long-term vacuum exposure and humidity exposure on properties of LP2 underfill were investigated to address potential reliability issues from exposure to space vacuum and terrestrial humid environments. The vacuum inside satellites operating at LEO is typically 10^{-6} to 10^{-7} Torr. Exposure to the vacuum environment induces outgassing of volatile components from polymers. The volatile components can contaminate sensitive optics and sensor surfaces. The outgassing can also result in the degradation of polymeric materials, especially at an elevated temperature. TMA, DMA, and lap shear samples were aged in a 10^{-7} Torr vacuum at +135°C to study the effect of long-term vacuum exposure. For humidity exposure, samples were exposed to 85% relative humidity at 85°C for seven days and 27 days.

2.2.1 Effect of long-term vacuum and humidity exposure to adhesive strength of the LP2 underfill

Adhesion of the underfill is known as the most important property for underfill reliability [1]. The underfill carries most of the stress from the CTE mismatch between the die and the substrate. If the underfill loses its adhesion, the stress cannot be properly dissipated to the underfill. An underfill cannot effectively reduce solder fatigue if there are cracks or delamination. Underfill cracking, underfill delamination, or chip cracking can take place if the underfill does not have proper adhesive strength. An underfill needs to be able to maintain adhesion after exposure to adverse environmental conditions such

as thermal cycling and/or moisture exposure. When exposed to a humid environment, epoxy materials can swell and lose adhesive strength [1, 2]. In order to investigate the effects of vacuum and humid environments on adhesive strength, lap shear samples of LP2 underfill were prepared. The thickness of the LP2 underfill in lap shear samples was about 120 µm. 0.06 inch thick aluminum was used as the panel material, bonded to LP2 material without applying primer.

A total of 30 lap shear samples were exposed to 85°C/85% relative humidity (RH). Fifteen samples were exposed for 168 hours, per level 1 condition of JEDEC standard J-STD-020D, and 15samples were exposed for 27 days, to investigate the effects of prolonged exposure to moisture.

Vacuum exposure was done on 15 samples in 6 to 9×10^{-7} Torr at 135°C for 80 days. Since the vacuum exposure was done at an elevated temperature, 15 samples were thermally aged at 135°C at atmospheric pressure for 30 days to isolate effects of the vacuum from the effects of thermal aging. Table 2.2.1-1 shows lap shear test results on various preconditioned samples. Five samples were tested at each condition. As-cured samples were tested only at the room temperature as a reference. Lap shear strengths of as-cured samples at −55°C and +125°C are available in our FY11 NEPP task report [1]. Lap shear strength of as-cured samples at room temperature in the FY12 study is significantly lower than in our FY11 report (3043 psi). This is because of the thickness of the panel in the FY11 experiment; at 0.12 inches, the thicker panel deflects less during the lap shear test, affecting the measurment. The results in Table 2.2.1-1 are valid for a comparative study. As shown in the Table 2.2.1-1, there was virtually no effect of vacuum exposure or thermal aging on adhesive strength of the LP2 material. However, the humidity exposure resulted in an approximately 30% decrease in lap shear strength. Lap shear strength of samples exposed to humidity for 27 days were almost the same as ones exposed for 168 hours, indicating that the adhesive strength will reach its minimum value within 168 hours. This indicates that exposure to humid environment may decrease thermal cycling life. However, unless experiments are done with actual packages, it is not certain how to estimate how the thermal cycling life of the package would be impacted by the humidity exposure.

Table 2.2.1-1. Lap shear strength of LP2 underfill exposed to different environmental conditions.

Sample condition	Lap shear strength (psi) at −55°C	Lap shear strength (psi) at +22°C	Lap shear strength (psi) at +125°C
As-cured		2050	
Vacuum thermal aged, 10^{-7} Torr, 135°C, 80 days	2125	2131	2164
Humidity exposed 85°C/85%, 168 hours	1853	1577	1481
Humidity exposed 85°C/85%, 27 days	1837	1576	1465
Thermal aged 135°C, 30 days	2182	2138	2615

2.2.2 Effect of long-term vacuum and humidity exposure to viscoelastic and thermal expansion behavior of the LP2 underfill

Figure 2.2.2-1 is TMA plots of four different types of LP2 underfill samples. Their preconditioning conditions are indicated in the plot. TMA was carried out using a TA Q400 TMA instrument with an expansion probe using a probe force of 0.0200 N. The cylindrical epoxy samples had a room temperature height (axial), measured by the Q400 quartz probe sensor, of ~2.4 mm, and a diameter (via micrometer) of 2.1 mm. The samples were equilibrated at the instrumental temperature lower limit of −150ºC, held isothermal for five minutes, followed by a temperature ramp to 225ºC at 3ºC/min. The TMA sample compartment was purged throughout the experiments using GN2 at 100 mL/min. CTEs are slopes of each curve. Tg is where transition in the slope takes place. Sudden shifts in the curve can be seen from the

humidity-exposed sample. The TMA measurement was done twice up to 220°C, but the shifts were still present. The shifts could be caused by the moisture exposure, but it is also possible that the shift is due to drift of the sample. Below Tg, all the samples showed similar CTE. The humidity-exposed sample exhibited slightly decreased CTE at temperatures above Tg, but the difference was not significant. Both vacuum thermal aged and thermal aged samples exhibited about 10 to 20°C increase in Tg. The Tg of humidity exposed sample seemed somewhat lower than the as-cured sample, but due to shifts in the curve it was impossible to determine the exact Tg.

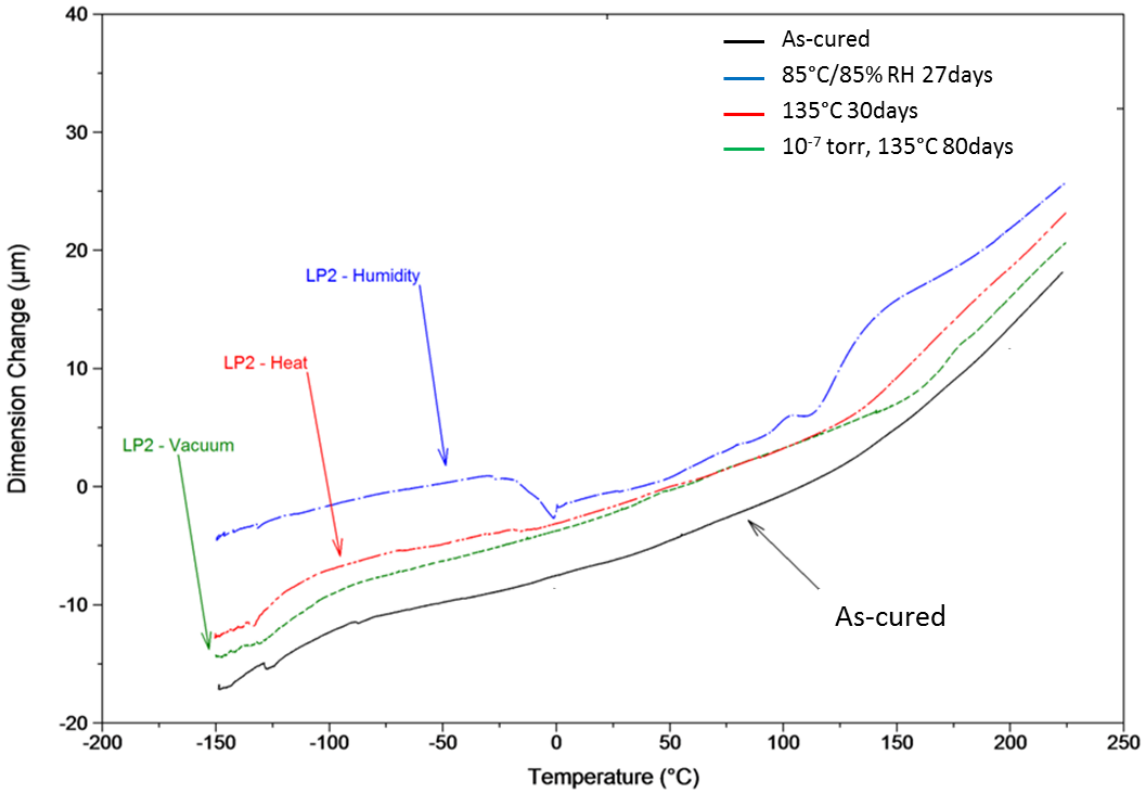

Figure 2.2.2-1. TMA plots of LP2 underfill material, exposed to different conditions

Figures 2.2.2-2 to 2.2.2-5 are DMA thermograms of LP2 underfill material exposed to different preconditioning. DMA was performed on a TA Q800 DMA instrument configured with a single cantilever clamp. DMA experiments were carried out from −145ºC (equilibrated and then held isothermal for five minutes) to +210ºC using a heat ramp rate of 2ºC/min, at a constant frequency (1 Hz) and constant amplitude (20 µm). The samples were in the shape of a regular rectangle approximately 38 mm long, 10mm wide and 2 mm thick, and used as-is. Sample length, a fixed value equal to the distance between the two clamp mounts, was 17.50 mm.

Storage modulus (E') inflection point, where a drop in E' takes place, is approximately Tg. As shown in Figures 2.2.2-2 to 2.2.2-5, both vacuum thermal aging and thermal aging resulted in an increase of Tg. The vacuum thermal aged sample exhibited higher Tg than the thermal aged sample. At this point, it is not clear whether this difference is due to longer exposure to heat or exposure to vacuum. Moisture absorption is known to cause a reduction of Tg [1]. For the humidity exposed LP2 sample, Tg can be almost 30°C lower than the as-cured sample, based on the temperature where the drop in E' took place.

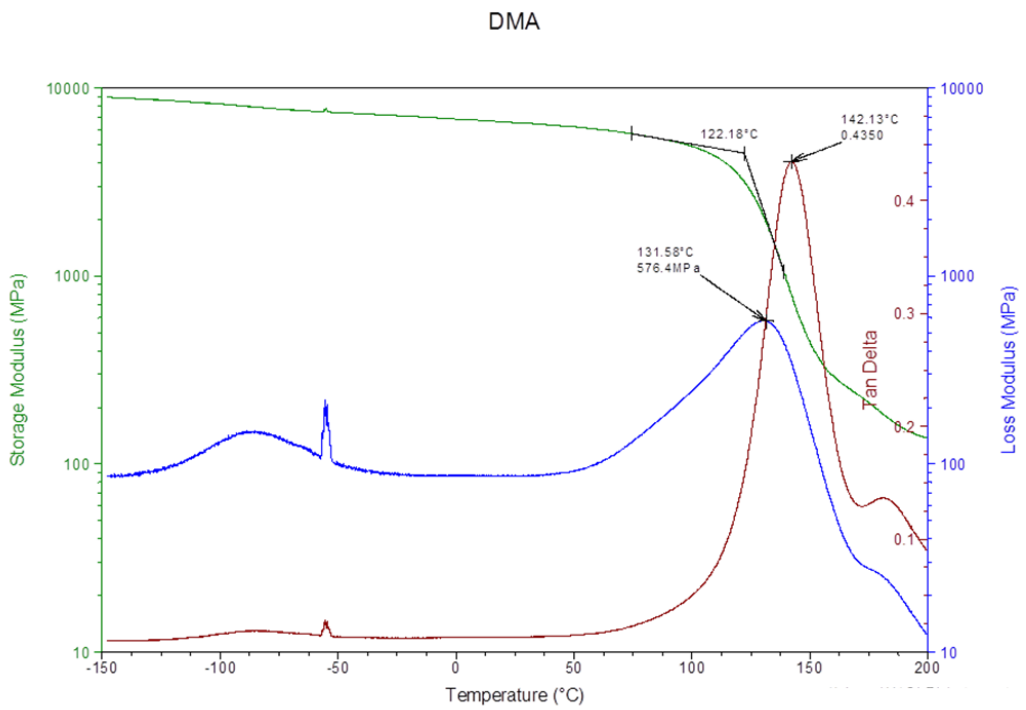

Figure 2.2.2-2. DMA plot of as-cured LP2 underfill material.

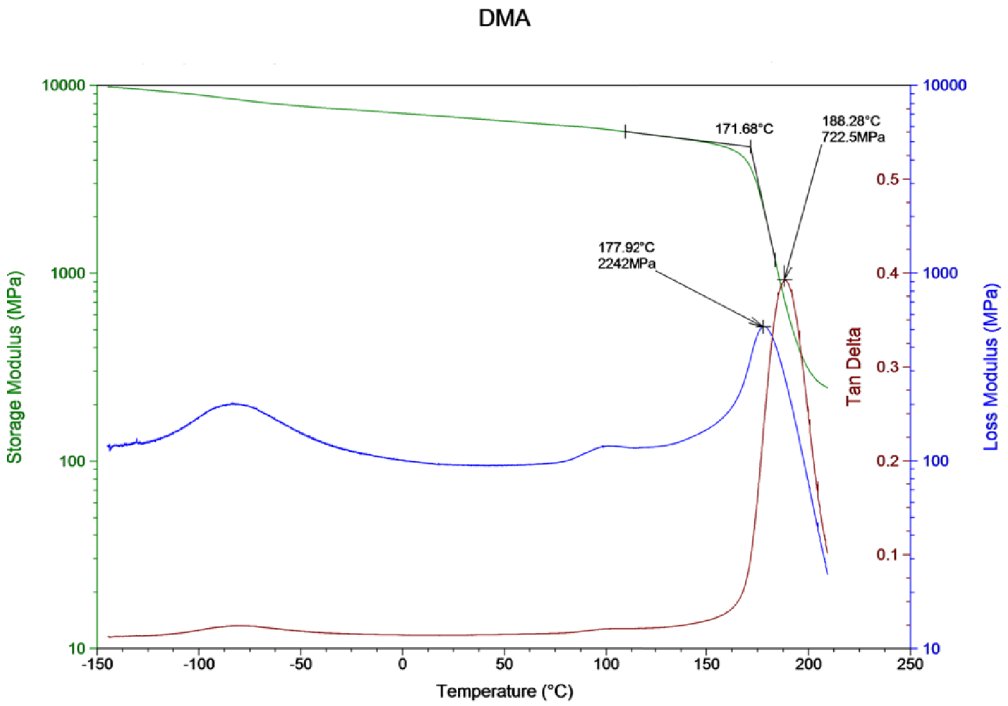

Figure 2.2.2-3. DMA plot of LP2 underfill material, aged in 10^{-7} Torr vacuum at 135°C for 80 days.

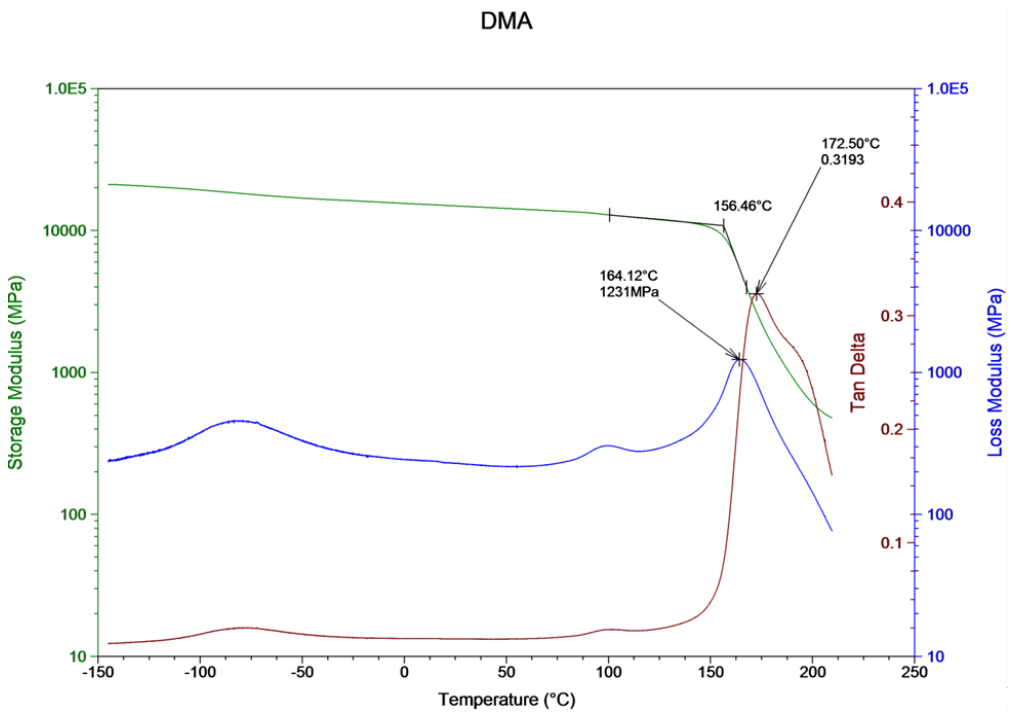

Figure 2.2.2-4. DMA plot of LP2 underfill material, aged at 135°C for 30 days.

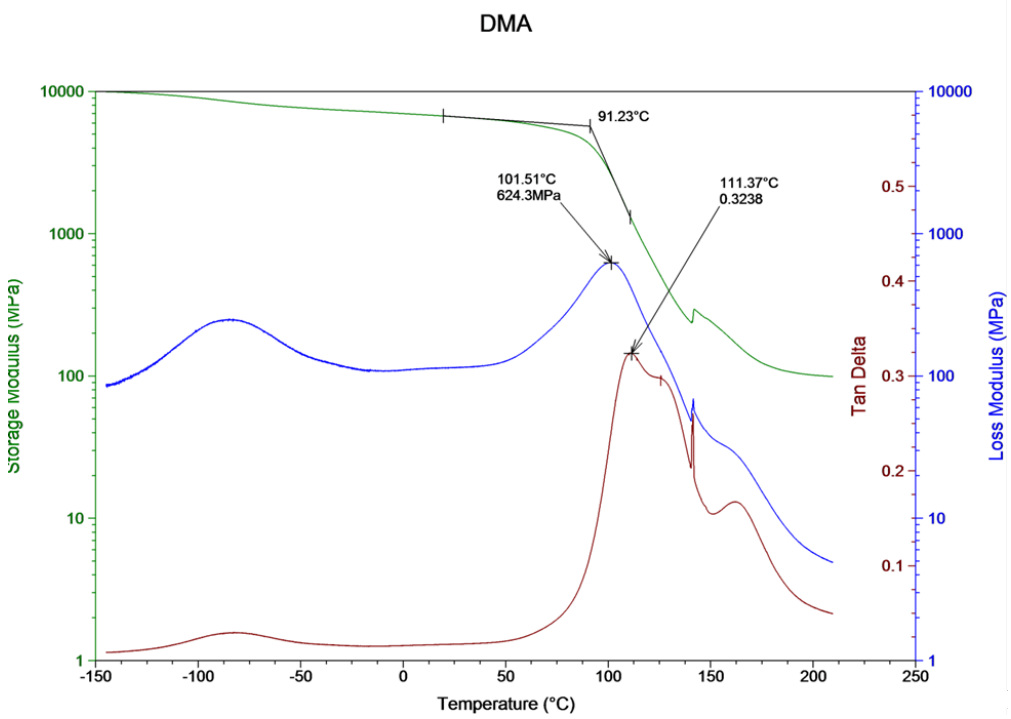

Figure 2.2.2-5. DMA plot of LP2 underfill material, exposed to 85°C/85% RH for 27 days.

3.0 PROPERTIES OF ATI LID ADHESIVE MATERIAL

The ATI lid adhesive material is a silver filled epoxy material used for attaching SiC heat spread on dies of V4 and V5. Same as the underfill material, the lid adhesive material will be directly exposed to the spacecraft and humid environment. We have conducted same tests on the ATI material as the LP2 material and investigated effect of long term vacuum exposure and humidity exposure. The effect of the long term vacuum exposure was conducted by aging various types of samples in 10^{-7} Torr vacuum at +135°C. For humidity exposure, samples were exposed to 85% relative humidity at 85°C for 7 days and 27 days.

3.1 Outgassing properties of the ATI material

Due to the non-hermeticity of the Xilinx packages, the underfill and lid adhesive materials are directly exposed to high vacuum, making outgassing of a concern. The outgassed component would contaminate sensitive devices. However, when considering the risk of contamination from the outgassing, the volume and the area of the material should also be taken into consideration. If a material has small volume and area, it will outgas only small amount of contaminant regardless of its outgassing characteristics. In the case of the LP2 underfill material, its volume is only about 0.08 cc (width×depth×height=2.54×2.54×0.012 cm^3), even if we do not consider volume of the flip chip solder bumps. Moreover, the exposed area of the underfill only about 0.12 cm^2 (width×height×4corners=2.54×0.012×4 cm^2). The lid adhesive material has even smaller thickness than the underfill material (25µm). It is little difficult to make a good assessment on total volume and area of the ATI material, because when the lid is attached to the die, a large portion of the ATI material is squeezed out and covers sides of the die. However, ATI material should have substantially smaller volume and area than the LP2 material. Therefore, risk of contamination from the outgassing of underfill and lid adhesive materials will always be low regardless of their outgassing characteristics, unless these types of packages are installed at the vicinity of sensitive devices. However, we have investigated outgassing properties of the ATI material to fully ensure that the material does not possess any outgassing issues.

Two types of specimens were analyzed: an as-cured specimen and a specimen thermal-vacuum conditioned for 12 hours at 135°C. The specimens were analyzed with Direct Analysis in Real Time (DART). DART is a non-vacuum, low-cost alternative test for collected vacuum condensable materials (CVCM). The analysis used the DART sampling system coupled to a high mass accuracy, time of flight Mass Spectrometer (DART-AccuTOF). The DART-AccuTOF system uses metastable Helium as surface ionization source. This enables molecules that are otherwise difficult to ionize and volatilize to be readily introduced into the mass spectrometer system. The system measures the parent ion of the molecule (M and/or M+1) with an accurate molecular weight of the desorbed compounds. The method determines the presence of vacuum-labile residues from plasticizers, additives and of uncured polymeric materials. The DART also provides a quantitative measure of the amount of vacuum labile residue that could condense as a CVCM. Based on experience, this is mainly in the 200 to 700 amu molecular weight range. The measurement is relative to a standard polypropylene material with a known CVCM of 0.08%. A collected vacuum condensable CVCM limit of 0.10% is generally recommended for flight materials.

The DART analysis results are shown in Table 3.1-1. The test indicated that the ATI material will have a low level of vacuum-labile residue relative to a reference material with a 0.08% CVCM. In addition, thermal-vacuum conditioning greatly lowered vacuum labile residues of the sample.

Table 3.1-1. Lap shear strength of ATI lid adhesive material exposed to different environmental conditions.

Sample	DART MS Total Ion Counts, 200–700 amu	Derived CVCM Equivalent
As-cured ATI	206K	0.08%
Thermal Vacuum aged ATI (10^{-7} Torr 135°C)	40K	0.015%

Sample	DART MS Total Ion Counts, 200–700 amu	Derived CVCM Equivalent
Reference PP, 0.08 CVCM	209K	0.08%

3.2 Effect of environmental exposure to properties of the ATI lid adhesive material

As with the LP2 underfill material, the ATI lid adhesive must also be expected to interact with the outside environment. In this report, the effects of long-term vacuum exposure and humidity exposure were investigated. The ATI material went through the same preconditioning as the LP2 material described in previous sections of the current report.

3.2.1 Effect of long-term vacuum and humidity exposure to adhesive strength of the ATI lid adhesive

Lap shear samples of ATI material were exposed to different environments before the lap shear test. Using 1 mil diameter glass beads as a spacer, thickness of the ATI material was set at 25 µm, to simulate the actual thickness of the ATI material in the V4/V5 packaging. 0.06 inch thick aluminum was used as the panel material, bonded with the ATI material without applying primer. Fifteen samples were tested without any preconditioning. Fifteen samples were exposed to 85°C/85% RH for 168 hours, per JEDEC standard J-STD-020D. Fifteen samples were exposed to 85°C/85% RH for 27 days to investigate the effects of prolonged exposure to humidity. Fifteen samples were stored in a 6 to 9×10^{-7} Torr vacuum at 135°C for 80 days to investigate the effects of long-term vacuum exposure. Fifteen samples were aged at 135°C for 30 days to isolate the effects of vacuum from the effects of thermal aging.

Table 3.2.1-1 shows lap shear test results of preconditioned lap shear samples of the LP2 material. Five samples were tested at each condition. Regardless of the preconditioning, the ATI material exhibited significantly reduced lap shear strength at +125°C, which was attributed to the fact that the Tg is well below +125°C.

Because the V4 and V5 devices generate greater heat than other FPGA devices, heat straps or heat pipes are often attached to the lid. The results imply that there can be potential delamination issues with the lid at elevated temperatures due to stress caused by the attached heat pipe.

Vacuum thermal aging and thermal aging did not show a noticeable effect on lap shear strength of the samples. However, the humidity exposure resulted in a significant decrease in the lap shear strength. While the LP2 material did not show difference in adhesive strength between samples exposed to humidity for 168 hours and 27 days, the ATI samples exposed to 27 days of humidity showed further decreased lap shear strength.

Table 3.2.1-1. Lap shear strength of ATI lid adhesive material exposed to different environmental conditions.

Sample condition	Lap shear strength (psi) at −55°C	Lap shear strength (psi) at +22°C	Lap shear strength (psi) at +125°C
As-cured	1985	2061	631
Vacuum thermal aged, 10^{-7} Torr, 135°C, 80 days	1855	1808	891
Humidity exposed 85°C/85%, 168 hours	1429	1366	452
Humidity exposed 85°C/85%, 27 days	225	1007	245
Thermal aged 135°C, 30 days	1796	1983	1049

3.2.2 Effect of long-term vacuum and humidity exposure to viscoelastic and thermal expansion behavior of the ATI lid adhesive material

Effects of environmental exposure to viscoelastic properties of the ATI material were investigated by conducting DMA measurements on preconditioned ATI material samples. DMA results are shown in Figures 3.2.2-1 to 3.2.2-4. As explained previously, temperatures where the E' drops or peaks of E" and Tanδ appear are all associated with Tg. Both vacuum thermal aging and thermal aging resulted in increase of Tg. The thermal aged sample showed two peaks of Tanδ, the second peak appeared at 143.42°C. For the humidity exposed sample, a temperature where E' drops was reduced to 21.43°C. However, DSC tests would be necessary in order to confirm Tg, becuase it is little unclear to determine exact Tg from the TMA results shown in Figure 3.2.2-5. The thermal aged ATI material exhibited two peaks of the tanδ, as can be seen in Figure 3.2.2-3. Often the tanδ having two peaks indicates formation of two phase solids and further investigation would be needed to clarify.

Figure 3.2.2-5 is a TMA plot of ATI material samples. CTEs of samples measured by TMA are summarized in Table 3.2.2-1. CTEs showed only little variation at temperatures below Tg, except for the humidity exposed sample. At temperatures above Tg, all the preconditioned samples showed reduced CTE compared to the as-cured sample.

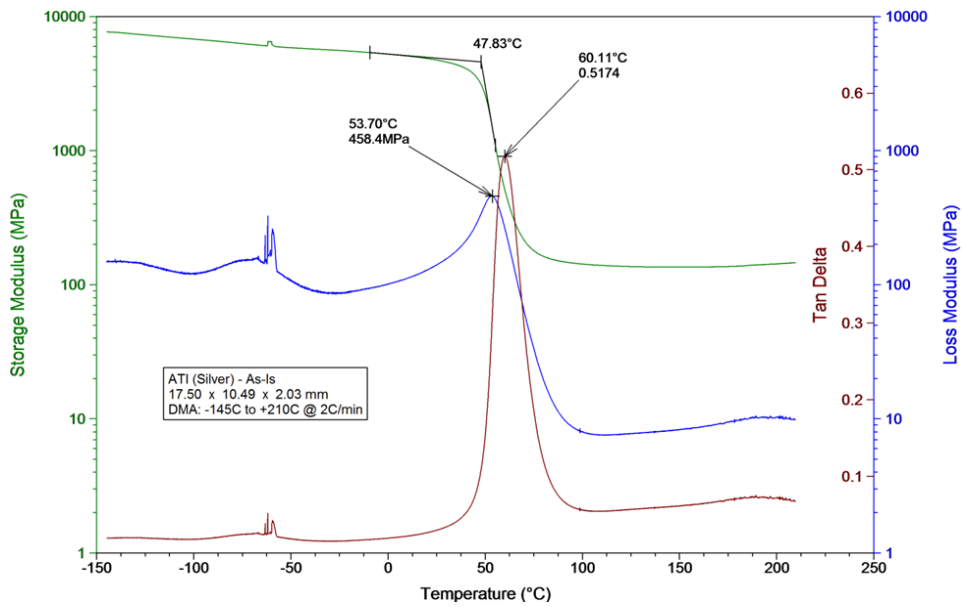

Figure 3.2.2-1 DMA thermogram of an as-cured ATI material sample.

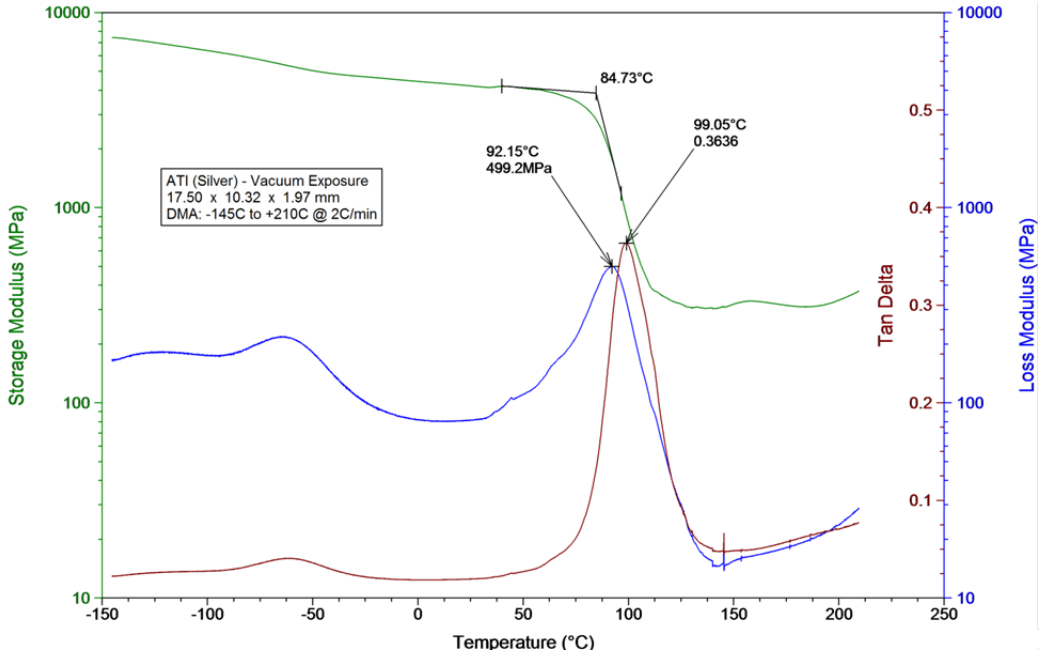

Figure 3.2.2-2 DMA thermogram of ATI material, aged in 10^{-7} Torr vacuum at 135°C for 80 days.

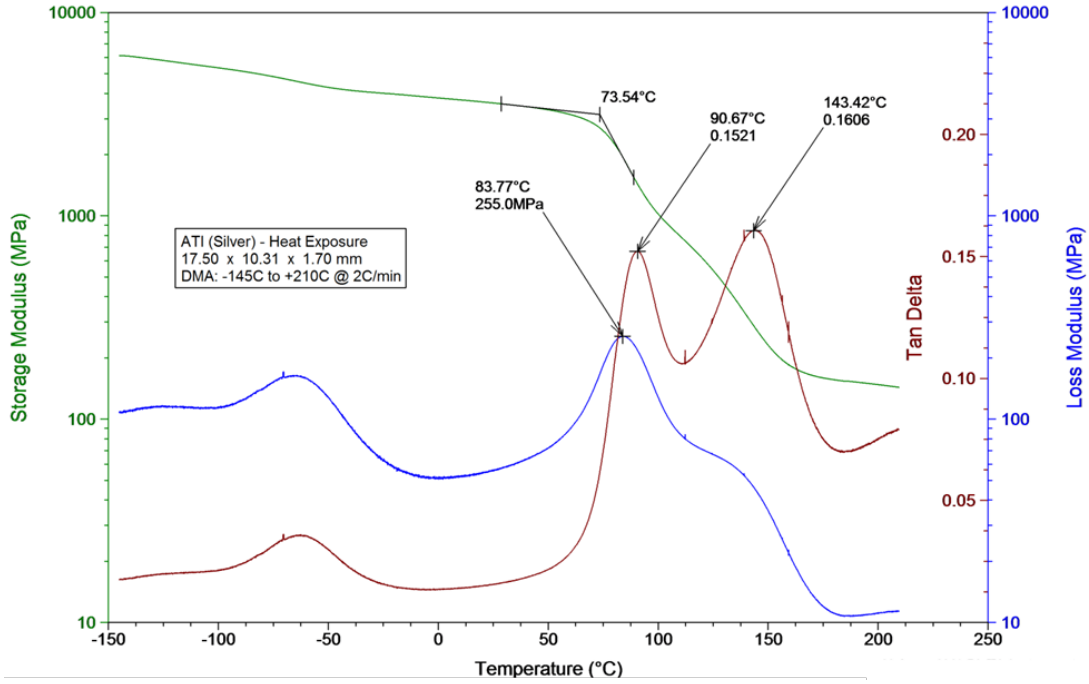

Figure 3.2.2-3 DMA thermogram of ATI material, aged at 135°C for 30 days.

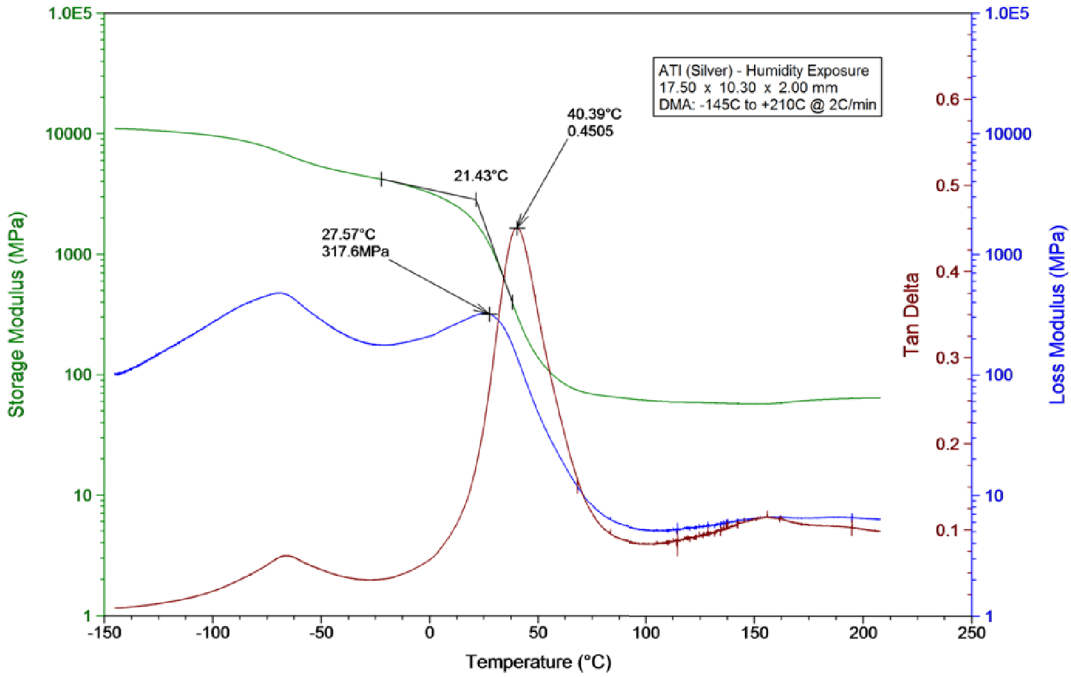

Figure 3.2.2-4 DMA thermogram of ATI material, exposed to 85°C/85% RH for 27 days.

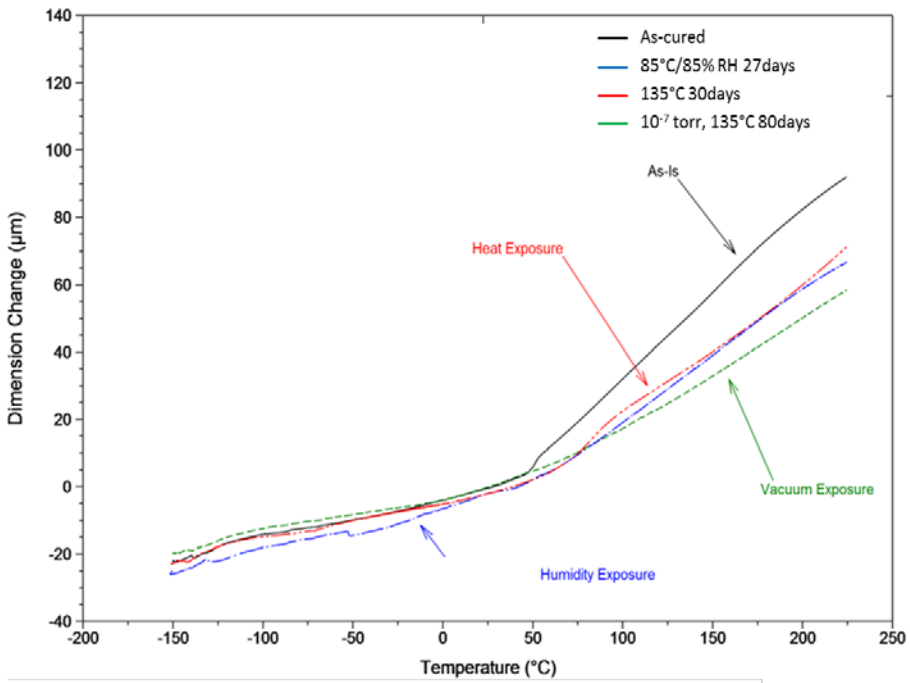

Figure 3.2.2-5. TMA plots of ATI material, exposed to different conditions

Table 3.2.2-1. CTE of ATI lid adhesive material exposed to different environmental conditions.

Sample condition	CTE below Tg (ppm/°C)	CTE above Tg (ppm/°C)
As-cured	42.29	183.1
Vacuum thermal aged, 10^{-7} Torr, 135°C, 80 days	41.37	139.1

Sample condition	CTE below Tg (ppm/°C)	CTE above Tg (ppm/°C)
Humidity exposed 85°C/85%, 27 days	50.99	163.1
Thermal aged 135°C, 30 days	43.31	154.9

3.2.3 Effect of long-term vacuum and humidity exposure to Thermal conductivity of the ATI material

Since the main function of the ATI material is to conduct heat from the die to the lid, effects of environmental exposure on its thermal conductivity was investigated. Thickness and thermal conductivity of the ATI materials are approximately 25 µm and 3 W/mK, respectively. And thickness and thermal conductivity of the SiC heat spread are approximately 2 mm and 250 W/mK, respectively. Both thickness and thermal conductivity of the ATI material are about 1% of those of the SiC heat spread. Therefore, although the ATI material is much thinner than the SiC lid, the ATI material and SiC heat equally contribute to the heat transfer from the die through the lid, because the heat transfer through conduction is proportional to the thermal conductivity and inversely proportional to the length of the material. The tests described here were performed to ensure that there is no significant drop in thermal conductivity after environmental exposures. Thermal conductivity of the ATI material was measured using a laser flash method. Samples were in a round disk shape, with 12.5 mm diameter and 2 mm thickness. The test results are summarized in Table 3.2.3-1. Samples with environmental exposures exhibited increased thermal conductivity compared to the as-cured sample, indicating that environmental exposure will not reduce thermal conductivity of the ATI material. The reduction of adhesive strength, discussed in the previous section, would be a more relevant issue, since overall heat transfer will be greatly impacted if voiding, delamination, or microcrack formation take place in the ATI material layer during the manufacturing or operation.

Table3.2.3-1. Thermal conductivity of ATI lid adhesive material exposed to different environmental conditions.

Sample condition	Thermal conductivity at +22°C (W/mK)	Thermal conductivity at +125°C (W/mK)
As-cured	2.34	2.92
Vacuum thermal aged, 10^{-7} Torr, 135°C, 80 days	3.58	4.05
Humidity exposed 85°C/85%, 27 days	2.94	2.91
Thermal aged 135°C, 30 days	4.29	4.28

4.0 SUMMARY

The Xilinx Virtex-4 QV (V4) and Virtex-5 QV (V5) are strong candidates for the next-generation FPGA for NASA applications. There have been concerns within the space community regarding the non-hermeticity of V4/V5 packages. Polymeric materials such as the underfill and lid adhesive will be directly exposed to the outside environment due to non-hermeticity. Even though a variety of reliability test data on V4/V5 packages are available, there are no test results on whether interaction between the mission environment and the polymeric materials will affect long term reliability of the package. During our previous FY11 task, among all the environmental concerns at LEO, the long-term vacuum exposure was rated as the most realistic environmental concern for V4/V5 type nonhermetic ceramic flip chip packages. Another concern was potential exposure to humidity at Earth prior to the launch. V4 and V5 share the same underfill (LP2) and lid adhesive material (ATI). In this study, the LP2 and ATI materials used in the V4/V5 packages were characterized to assess potential reliability concerns. The task mainly focused on investigating how properties of LP2 and ATI changed according to temperature and exposure to different environments.

The long-term vacuum exposure did not degrade properties of the LP2 material. However, the LP2 material exhibited significantly reduced elastic modulus at +125°C, and also exhibited reduced adhesive strength after exposure to moisture. The ATI material also did not show any degradation after exposure to a long-term vacuum. However, it exhibited significantly reduced adhesive strength at +125°C and after exposure to moisture.

5.0 REFERENCES

[1] J.O. Suh and R.P. Dillon, "Xilinx V4 package reliability: properties and reliability of LP2 underfill material," FY11 NASA Electronic Parts and Packaging (NEPP) Program task report, 2012.

[2] Personal communication, Scott Popelar, Aeroflex Corporation.

[3] S.L. Buchwalter, M.E. Edwards, D. Gamota, M.A. Gaynes, and S.K. Tran, "Underfill: The Enabling Technology for Flip-Chip Packaging," in *Area Array Interconnection Handbook*, eds. K. J. Puttlitz and P. A. Totta, Springer, 2001.

[4] T. Ferguson and J. Qu, "Effect of moisture on the interfacial adhesion of the underfill/solder mask interface," in *Transactions of ASME*, vol. 124, pp. 106–110, 2002.

[5] T. Ferguson and J. Qu, "The effect of moisture on the adhesion and fracture of interfaces in microelectronic packaging," in *Micro- and Opto-Electronic Materials and Structures: Physics, Mechanics, Design, Reliability, Packaging*, eds. E. Suhir, Y. C. Lee, and C. P. Wong, 2007, pp B431–B471.

[6] E.L. Mckague, J.D. Reynolds, and J.E. Halkias, "Swelling and glass-transition relations for epoxy matrix material in humid environments," *J. Appl. Polym. Sci.*, vol. 22, no. 6, pp. 1643–1654, 1978.